

Restore from Restored: Single-image Inpainting

Eunhye Lee*, Jeongmu Kim*, Jisu Kim*, Tae Hyun Kim†

Dept. of Computer Science, Hanyang University
Seoul, South Korea

{dldms1345, jmkim1503, atat1270, taehyunkim}@hanyang.ac.kr

Abstract

Recent image inpainting methods have shown promising results due to the power of deep learning, which can explore external information available from the large training dataset. However, many state-of-the-art inpainting networks are still limited in exploiting internal information available in the given input image at test time. To mitigate this problem, we present a novel and efficient self-supervised fine-tuning algorithm that can adapt the parameters of fully pre-trained inpainting networks without using ground-truth target images. We update the parameters of the pre-trained state-of-the-art inpainting networks by utilizing existing self-similar patches (i.e., self-exemplars) within the given input image without changing the network architecture and improve the inpainting quality by a large margin. Qualitative and quantitative experimental results demonstrate the superiority of the proposed algorithm, and we achieve state-of-the-art inpainting results on publicly available benchmark datasets.

Introduction

Image inpainting, an image post-processing technique that removes unnecessary parts of images, such as subtitles and obstacles, and fills these areas with new colors and textures. Inpainting has extensive applications in areas of photo editing, restoration, and even video editing (Barnes et al. 2009; Levin et al. 2004; Yu et al. 2019; Kim et al. 2019), and the main goal is to generate plausible images that are semantically consistent with the overall context and to fill the missing area to be continuous with the surrounding area.

Many traditional inpainting approaches based on the diffusion technique compute pixel values of the missing area using pixel values in the surrounding area (Bertalmio et al. 2000; Ballester et al. 2001). Although diffusion-based approaches are effective in recovering small areas (e.g., subtitle removal), they produce blurry results when the missing area is large (e.g., object removal). As an alternative, patch-match-based methods have been proposed to locate similar patches within the given image and copy intensity values of these similar patches into the missing area (Liang et al. 2001; Hays and Efros 2007; Barnes et al. 2009). These methods can fill the missing area with realistic contents using the information within the input image. However, they cannot re-

*These authors contributed equally.

†Tae Hyun Kim is corresponding author.

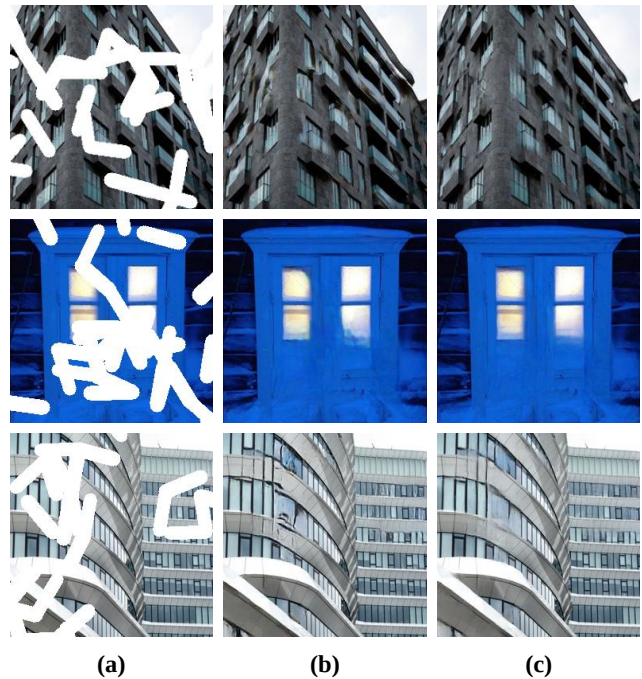


Figure 1: Our fine-tuning results with numerous inpainting networks. (a) Masked input images. (b) Initially restored results from pre-trained inpainting networks in the order of GatedConv (Yu et al. 2019), EdgeConnect (Nazeri et al. 2019), and GMCNN (Wang et al. 2018). (c) Our fine-tuning results.

store faces or complex landscapes that require information outside the input image.

The development of deep learning technologies has remarkably improved the performance of image inpainting techniques and made it possible to reconstruct considerably challenging images. First, context encoders pioneered the use of deep neural networks in the image inpainting task and introduced an architecture composed of convolutional encoder and decoder with adversarial loss (Pathak et al. 2016; Goodfellow et al. 2014). The encoder computes a latent feature representation from the input image and the decoder uses the feature representation to restore pixels in the missing area, consequently inferring and reconstructing the overall structure of the input image. The

output demonstrates a realistic texture as it approaches the distribution of the real image through the adversarial loss. Follow-up studies carry out various attempts while maintaining encoder-decoder structures with discriminators, presented in the work of context encoders. Among them, attention modules are exploited to generate realistic textures (Yu et al. 2018; Ren et al. 2019; Li et al. 2020). These attention modules allow searching non-local regions to utilize information among similar structures in the given input image and fill pixel values of missing areas. Some studies perform structural restoration before carrying out the inpainting to clarify the boundary of the missing hole (Ren et al. 2019; Nazeri et al. 2019; Xiong et al. 2019).

Although these neural approaches trained in a supervised manner with a large external training dataset for the inpainting task have shown promising and satisfying results, they have difficulties in fully utilizing the information within given test images. Thus, we propose a new self-supervised learning approach to utilize internal statistics available within the given input test image such as patch-recurrence to overcome this limitation. Patch-recurrence is a property that many similar patches are existing within a single natural image and it is utilized in numerous image restoration techniques including image denoising, inpainting, and super-resolution (Michaeli and Irani 2014; Glasner, Bagon, and Irani 2009; Huang, Singh, and Ahuja 2015). In image inpainting, Deep Image Prior (DIP) (Ulyanov, Vedaldi, and Lempitsky 2018) exploits self-similarity at the test time by training a randomly initialized neural network in a self-supervised manner. However, its inpainting results highly depending on the selection of hyper-parameters, particularly for a large mask. Moreover, DIP is limited in generating plausible objects because it cannot exert the power of deep learning through large external datasets.

To alleviate these problems, we develop a new learning algorithm that combines supervised and self-supervised approaches to benefit from both the external dataset and the given input test image. This approach improves the performance of existing state-of-the-art inpainting networks by simply updating network parameters using the internal information (i.e., repeating structure/texture and color distribution) available from the given input image at test time. Specifically, we use parameters of fully pre-trained inpainting networks on a large external dataset as initial values. We then fine-tune the network parameters in a self-supervised manner at the test stage by exploiting self-exemplars within the input test image and produce improved results as shown in Figure 1. Note that broken lines and crushed edges in the initial results are clearly improved, and the original shapes are properly restored with the proposed fine-tuning algorithm. Moreover, our learning method is not restricted to specific network architecture and can be applied to various conventional networks and can easily upgrade the parameters of the conventional inpainting networks without changing their original architectures.

The main contributions are summarized as follows:

- A novel self-supervised fine-tuning method that exploits recurring patches within the test image is proposed.

- Superior inpainting results on benchmark datasets are achieved by utilizing both internal and external datasets.
- Our approach can be applied to various inpainting networks without modifying their original network architecture and loss functions.

Related Work

Image inpainting

Recently, deep learning methods have shown successful results in image inpainting. By learning the information of large external datasets, they overcome the limitation of traditional methods of trying to create unique content, such as human faces or complex scenes (Bertalmio et al. 2000; Barnes et al. 2009; Huang et al. 2014). Context encoder (Pathak et al. 2016) introduces an encoder-decoder network to extract the semantics of the image based on GAN to generate realistic details. Jiahui Yu (2018) propose the contextual attention module to exploit image contents far from the hole. The module finds the most similar background patches with pixels of the missing area which are estimated in advance by a coarse network to reconstruct the missing area. Generative multi-column CNN (Wang et al. 2018) uses parallel networks with different receptive field sizes to prevent the error propagation caused by the coarse and fine networks that are connected in series. Guilin Liu (2018) proposed the use of partial convolution to learn various forms of masks, not only squared masks. The partial convolution layer performs the mask update and weight re-normalization of the masked area to propagate only valid information of the input. In a similar approach by Jiahui Yu (2019), gated convolution automatically finds a proper mask for the input and considers the gating value calculated across a spatial location of every layer and channel. EdgeConnect (Nazeri et al. 2019) introduces a two-stage inpainting network model that first generates the edge map and then recovers the whole image. However, this model is limited by its inability to utilize additional useful information, such as image color. StructureFlow (Ren et al. 2019) uses a smooth image while preserving the edges obtained via RTV (Xu et al. 2012) instead of the edge map and employs appearance flow module (Zhou et al. 2016) to achieve an attention effect for realistic texture. Jingyuan Li (2020) presented recurrent feature reasoning (RFR) network that fills the missing area gradually to cover large holes using the knowledge consistent attention.

Self-supervised learning for restoration

The self-supervised approach for image restoration primarily refers to the training of the neural networks using only information from the input images themselves without corresponding clean images (Lehtinen et al. 2018; Batson and Royer 2019; Shocher, Cohen, and Irani 2018). For the inpainting task, Deep Image Prior (Ulyanov, Vedaldi, and Lempitsky 2018) trains a simple CNN using the internal statistics such as patch-recurrence and obtains the improved result without the ground-truth image. However, these methods can only utilize internal data because they train the network from random scratch at the test time.

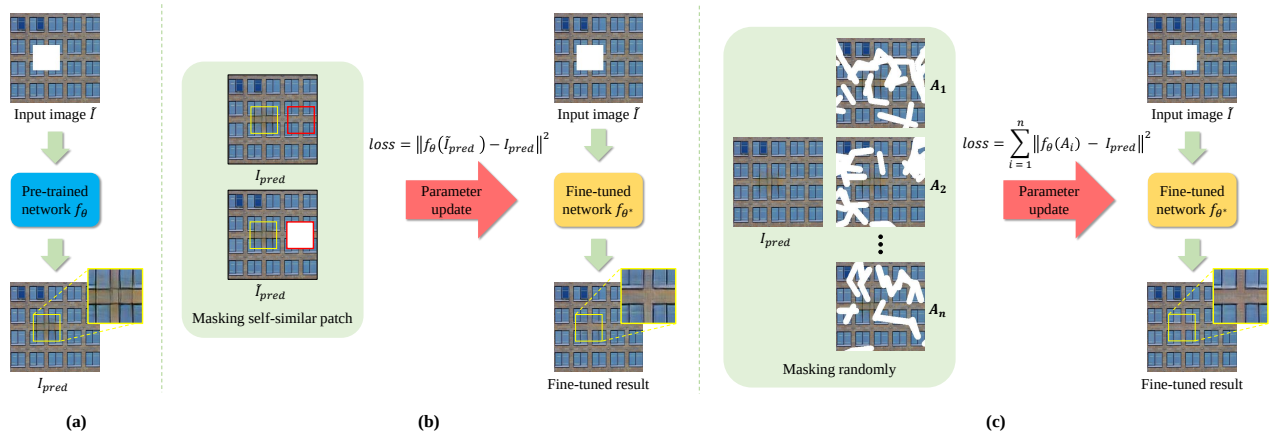


Figure 2: Inpainting results by EdgeConnect (Nazeri et al. 2019) before and after fine-tuning. (a) Fully pre-trained EdgeConnect produces artifacts. (b) Fine-tuned EdgeConnect using a corresponding patch (red box) within the input can remove artifacts. (c) Fine-tuned EdgeConnect using randomly masked input can also remove artifacts without finding correspondences.

In contrast, we not only exploit the internal information in the test input image but also utilize the information from the large external dataset similar to (Park et al. 2020; Lee et al. 2021) to overcome the limitation of the self-supervised approach that cannot exert the power of deep learning via large external datasets.

Proposed Method

In this section, we introduce a simple, yet effective self-supervised learning approach to adapt the parameters of pre-trained inpainting networks to the given input image.

Patch-recurrence for inpainting

The internal information available within the input image is very important for the image inpainting task and should be considered to generate semantically consistent and realistic results when filling missing areas. Images generally demonstrate the property of patch recurrence, which enables the repeated presentation of many identical or similar patches in a single image. The information of similar patches inside the image is used in past patch-match-based methods (Darabi et al. 2012; Barnes et al. 2009; Huang et al. 2014) and recent deep-learning methods with the attention mechanism (Yu et al. 2018; Ren et al. 2019; Li et al. 2020). Patch-match-based approaches find similar patches within the input to fill the hole and paste them. By comparison, the attention module (Yu et al. 2018; Li et al. 2020) and appearance flow (Ren et al. 2019) in deep approaches find similar patches/features in the given input image corresponding to the target (missing) area, and resulting attention maps are used to complete the texture within that area. These methods improve the inpainting results by exploiting the internal information during test time by using additional network modules (e.g., non-local operator) to compute attention maps. However, the search space of these modules for matching is relatively limited in practice, and cannot fully exploit the input image.

Therefore, we introduce a new approach that can fully utilize the recurring patches in the given input and also present

a new self-supervised fine-tuning method that enhances the quality of inpainting results of existing networks using these self-exemplars.

Patch-match-based inpainting without explicit patch-match

Existing learning-based inpainting methods learn how to reconstruct the missing area using a large number of training images during the training phase. However, the input image given at the test phase may include unique and unseen information, such as unusual structures, textures, and colors, which are rare in the training dataset. In this case, the pre-trained networks may generate unnatural outputs incompatible with the specific pattern in the background. Therefore, we propose a new inpainting approach to exploit the specific information available within the input test image by utilizing multiple similar patches in the input and further improve the pre-trained networks by adapting the network parameters to the specific input image.

We illustrate how self-similar patches can be used to fine-tune the network parameters and improve the performance of conventional inpainting networks. In Figure 2(a), we first obtain an initial inpainting result I_{pred} by applying the fully pre-trained EdgeConnect (Nazeri et al. 2019) network f_θ to an input image \tilde{I} distorted with a squared mask. Next, in Figure 2(b), we generate a newly masked image \tilde{I}_{pred} to utilize repeating structures of the given input by removing a self-similar patch in I_{pred} (red squared region). Then, by minimizing the MSE between I_{pred} and the restored image $f_\theta(\tilde{I}_{pred})$ from the newly masked image \tilde{I}_{pred} , we can fine-tune the network parameters θ to θ^* . Accordingly, we can update network parameters to the input image and can improve the performance of the inpainting network. Note that we adapt network parameters without using the ground-truth image during the fine-tuning. In Figure 2(c), we show that we can also fine-tune the network by corrupting the initially restored image with random masks without explicit patch-match to find self-similar patches. Specifically, we gener-

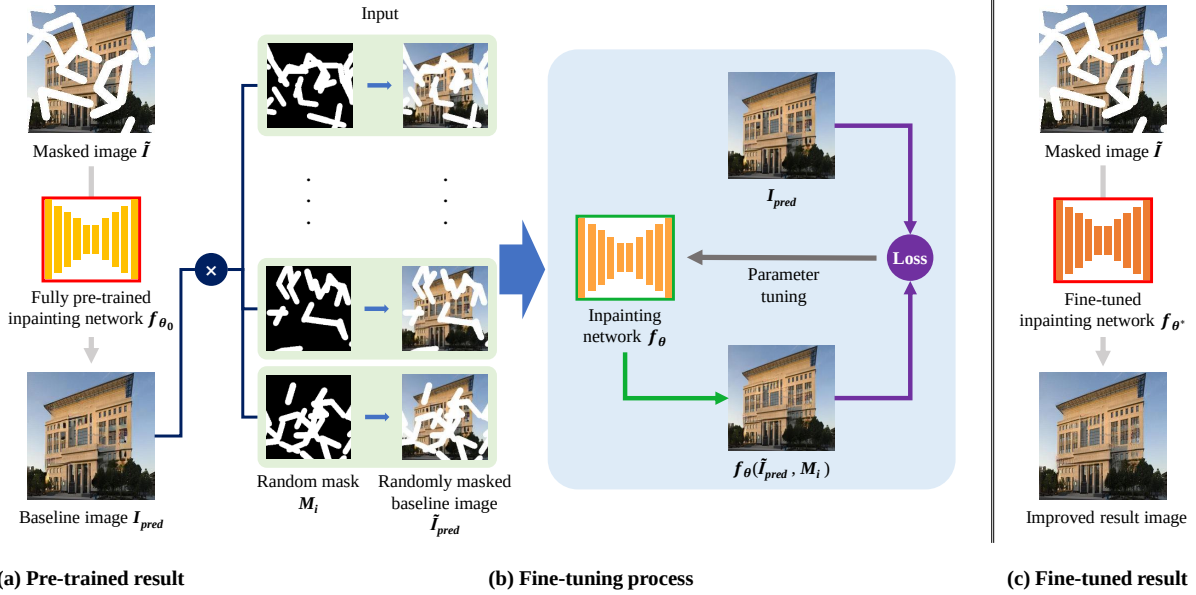


Figure 3: Overall flow of the proposed fine-tuning mechanism. (a) Initial inpainting result from the masked input image using the pre-trained network. (b) Fine-tuning with random masks on the result from the baseline network. (c) Fine-tuned network produces an improved result consistent with the input image.

ate multiple training images for fine-tuning by corrupting I_{pred} using random masks, then fine-tune the network by minimizing MSE between the initial inpainting result I_{pred} and the restored image $f_{\theta}(A_i)$ from the newly corrupted image A_i . By doing so, we demonstrate that we can adapt network parameters without explicitly searching for self-similar patches within the input as in Figure 2(b).

Conventional methods require dedicated algorithms and specialized network modules to search similar patches explicitly (Barnes et al. 2009; Darabi et al. 2012; Yu et al. 2018; Ren et al. 2019). In contrast, we learn the self-exemplars by using the randomized masking (corruption) scheme during the test phase without any additional algorithm or network modules to find similar patches (e.g., patch-match). As the area of similar patches can be randomly masked several times during the randomized masking scheme, these self-similar patches can be naturally exposed to the network during the fine-tuning stage. Thus, the inpainting network can learn to restore the missing area using similar patches, as shown by the result of Figure 2(c), which shows similar improvements to Figure 2(b). Notably, another advantage of this approach is that the randomized-masking-based fine-tuning mechanism does not restrict the shape, size, and number of the recurring patches in the input.

Overall flow

The overall flow of the proposed fine-tuning approach is described in Algorithm 1 and illustrated in Figure 3.

We first start the fine-tuning process with the initially restored image I_{pred} by using the fully pre-trained inpainting network as follows:

$$I_{pred} = f_{\theta_0}(\tilde{I}, M), \quad (1)$$

where θ_0 denotes the fully pre-trained parameters of the baseline inpainting network f and \tilde{I} denotes the masked input image. A binary map M denotes a given input mask where missing and other areas are represented by 1 and 0.

Second, we acquire a training dataset using the initially restored image I_{pred} . We generate a randomly corrupted masked image for the i_{th} fine-tuning iteration as follows:

$$\tilde{I}_{pred} = I_{pred} \odot (1 - M_i), \quad (2)$$

where M_i denotes the randomly generated binary mask and \odot represents the element-wise multiplication. The newly synthesized masked image \tilde{I}_{pred} and initially restored image I_{pred} become the input and target of our training dataset. We render a restored image $I_{pred(\theta)}$ from the newly masked image \tilde{I}_{pred} using the inpainting network f_{θ} .

Third, we compute gradient values with respect to network parameters using the predefined loss functions used in pre-training the baseline inpainting network and then update network parameters using a conventional optimizer (e.g., ADAM), and the loss is computed using I_{pred} and $I_{pred(\theta)}$. Notably, if the baseline inpainting network includes GAN architecture, the discriminator of GAN computes the adversarial loss by using I_{pred} as the real sample since the ground-truth clean image is not available.

For instance, for the pixel-wise loss (i.e., reconstruction loss), we can use the L2 loss function as follows:

$$loss_{rec}(\theta) = \|I_{pred} \odot (1 - M) - I_{pred(\theta)} \odot (1 - M)\|^2. \quad (3)$$

In practice, to compute the reconstruction loss, we exclude the part corresponding to the original mask M (i.e., initially restored area) since we see improvements in our experiments by making this slight modification. Note that we can use

Algorithm 1: Fine-tuning algorithm

Input: input masked image \tilde{I} , original mask M

Require: inpainting network f and the pre-trained parameter θ_0 , number of training T , random masks $\{M_i\}$, learning rate α

Output: enhanced inpainting result $f_{\theta^*}(\tilde{I}, M)$

```
1:  $i \leftarrow 0$ 
2:  $\theta \leftarrow \theta_0$ 
3:  $I_{pred} \leftarrow f_{\theta_0}(\tilde{I}, M)$ 
4: while  $i < T$  do
5:    $\tilde{I}_{pred} \leftarrow I_{pred} \odot (1 - M_i)$ 
6:    $I_{pred(\theta)} \leftarrow f_{\theta}(\tilde{I}_{pred}, M_i)$ 

   // Random transformations can be applied for the loss
7:    $loss_{rec}(\theta) \leftarrow \|I_{pred} \odot (1 - M) - I_{pred(\theta)} \odot (1 - M)\|^2$ 

8:    $loss_{adv}(\theta) \leftarrow VGG \text{ and/or adversarial losses}$ 
9:    $Loss(\theta) \leftarrow loss_{rec}(\theta) + loss_{adv}(\theta)$ 

   // Parameter update
10:   $\theta \leftarrow \theta - \alpha \nabla_{\theta} Loss(\theta)$ 
11:   $i \leftarrow i + 1$ 
12: end while
13:  $\theta^* \leftarrow \theta$ 
14: Return:  $f_{\theta^*}(\tilde{I}, M)$ 
```

any conventional reconstruction losses (e.g., L1). Moreover, when considering additional losses, such as VGG and adversarial losses, we do not need to make any modifications. We employ the original loss functions used to pre-train the baseline inpainting networks, and the expression is $loss_{adv}(\theta)$. Thus, the overall loss function that updates parameters of the given inpainting network is expressed as follows:

$$Loss(\theta) = loss_{rec}(\theta) + loss_{adv}(\theta). \quad (4)$$

Then, we repeat these steps T times. Notably, random transformations can be applied during fine-tuning to prevent the network from producing I_{pred} regardless of its input.

Finally, the network parameter is upgraded to θ^* , and we obtain the final fine-tuned image $f_{\theta^*}(\tilde{I}, M)$ with the original input image \tilde{I} and mask M .

Experimental result

Please refer to our supplementary material for more results, and the code will be publicly available upon acceptance.

Implementation details

To evaluate the performance of the proposed fine-tuning algorithm, we use three different inpainting networks, GatedConv (Yu et al. 2019), EdgeConnect (Nazeri et al. 2019), and GMCNN (Wang et al. 2018), as baseline networks of our algorithm. The experiments are performed using the official code for each model.

For our experiments, we use officially available and fully pre-trained network parameters on the Places2 dataset (Zhou et al. 2017) for each network and fine-tune the pre-trained parameters via the proposed method in Algorithm. 1. We

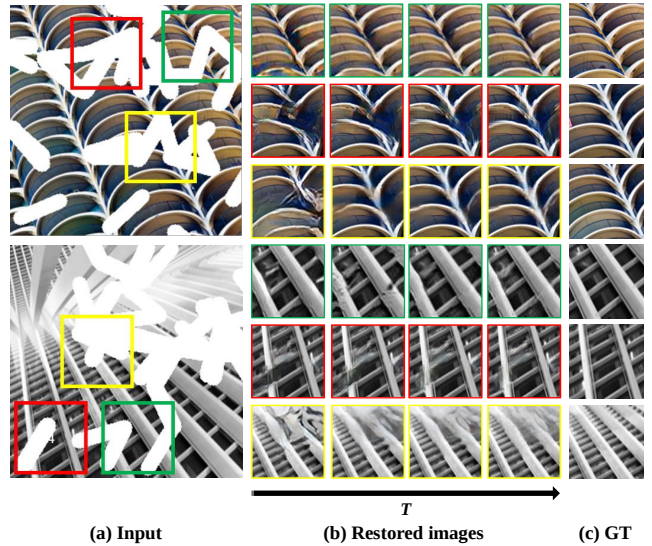


Figure 4: Visual results on the Urban100 dataset according to the fine-tuning progress. Green, red, and yellow boxes represent the results by GatedConv, EdgeConnect, and GMCNN, respectively. (a) Input masked images. (b) Initially restored image and fine-tuned images for T iterations. **Green box:** GatedConv results (From left to right: $T=0$, $T=100$, $T=200$, $T=400$). **Red box:** EdgeConnect results (From left to right: $T=0$, $T=100$, $T=500$, $T=1000$). **Yellow box:** GMCNN results (From left to right: $T=0$, $T=50$, $T=150$, $T=200$). (c) Ground-truth images.

evaluate the performance of the proposed algorithm on test sets in conventional benchmark datasets, such as Places2 and Urban100 (Huang, Singh, and Ahuja 2015). The Places2 dataset is a mixed dataset of people, landscapes, and buildings; the Urban100 dataset mainly consists of buildings with repetitive patterns. We use the random free-form masks for fine-tuning introduced in (Yu et al. 2019). The input image size for the fine-tuning is 256×256 and each input image includes holes covering approximately 20% to 40% of the image. We utilize the same optimizer and loss function used in each of the pre-trained models, but we modify the learning rate for the fine-tuning: we use learning rate of 10^{-5} for EdgeConnect and GatedConv, and 10^{-4} for GMCNN.

Our experiments are conducted with Intel i9 and NVIDIA RTX2080 Ti GPU, and it takes 0.2, 0.3, and 0.7 seconds to perform 1 fine-tuning iteration (patch-size = 256×256 , batch-size = 4) with GMCNN, GatedConv, and EdgeConnect respectively.

Ablation study

Number of fine-tuning iterations T and image quality
In Figure 4, we show changes in image quality depending on the number of fine-tuning iterations. The structure of the resulting image is gradually improved as fine-tuning progress.

However, we sometimes observe unexpected artifacts when T is very small since networks can not fully utilize the self-similar patches, and see over-fitted and blurry images when T is very large. Thus, we need to determine the optimal fine-tuning iterations to produce the best results, and we

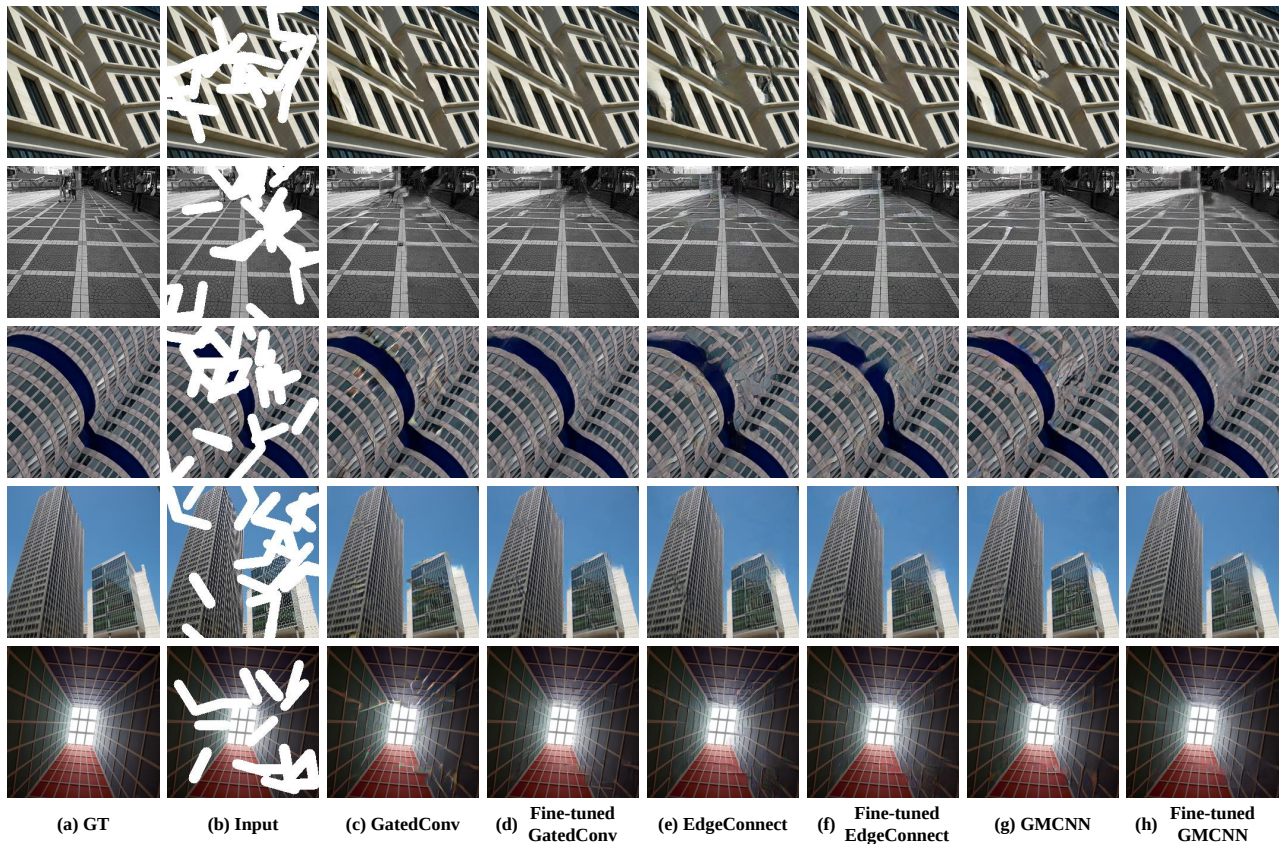


Figure 5: Qualitative comparison of results on the Urban100 dataset. From left to right: ground-truth, the masked input image, three image pairs of before and after fine-tuning each model.

use the Fréchet inception distance (FID) (Heusel et al. 2017) which can measure the image quality without the ground-truth clean image. Specifically, we compute FID score at each iteration and stop the fine-tuning when it starts to increase. We find that FID values are highly consistent with human judgment for the quality of images produced by the same image. Please refer to the supplementary for more details. In the remaining experiments, we use the fixed number of iterations based on this manner, and around 400, 1000, and 200 iterations for each pre-trained model (i.e., Gated-Conv, EdgeConnect, and GMCNN) are best on average.

Quantitative results

We quantitatively evaluate the performance of fine-tuned networks with peak signal-to-noise ratio (PSNR), and structural similarity index measure (SSIM) to compare the inpainting results objectively. These methods mainly measure the distortion of the results, assuming that the ideal results are the same as the original. Moreover, we compare the perceptual quality of the results by comparing FID and LPIPS (Zhang et al. 2018), and we use AlexNet (Krizhevsky 2014) to compute LPIPS in this study.

Table 1 and Table 2 list the quantitative restoration results. First, Table 1 shows the comparison of the results from each fine-tuning iteration on the Places2 dataset. One thou-

Model	# iter. (=T)	PSNR	SSIM	FID	LPIPS
Gated Conv	0 (baseline)	23.25	0.8831	73.93	0.103
	100	23.10	0.8767	77.22	0.109
	200	23.36	0.8820	73.55	0.103
	400	23.76	0.8890	72.82	0.097
	1000	23.97	0.8913	79.08	0.101
Edge Connect	0 (baseline)	24.00	0.8934	28.06	0.098
	100	24.04	0.8941	27.94	0.098
	200	24.06	0.8946	27.78	0.097
	400	24.09	0.8950	27.57	0.097
	1000	24.12	0.8957	27.23	0.096
GMCNN	0 (baseline)	23.79	0.8477	69.92	0.078
	100	24.70	0.8586	65.56	0.077
	200	24.61	0.8550	61.60	0.069
	400	24.47	0.8488	67.44	0.070
	1000	24.18	0.8439	75.13	0.082

Table 1: Fine-tuning results of various inpainting models on the Places2 dataset by changing the number of iterations.

sand images from the Places2 test dataset are used for the evaluation. With the aid of our fine-tuning algorithm, overall metrics values improve consistently compared with the restoration results by the pre-trained baseline models (i.e., T=0). Next, Table 2 presents the improvements between the results of pre-trained models and the outcomes after fine-

	GatedConv	EdgeConnect	GMCNN
PSNR*	21.38 → 22.64	22.73 → 23.19	21.64 → 23.38
SSIM*	0.862 → 0.888	0.880 → 0.892	0.830 → 0.851
FID[†]	75.34 → 58.80	53.98 → 45.34	77.96 → 70.83
LPIPS[†]	0.096 → 0.078	0.085 → 0.073	0.083 → 0.082

Table 2: Comparisons between results before and after fine-tuning of each baseline model on Urban100 dataset. Lower [†] and higher * scores indicate better quality of images.

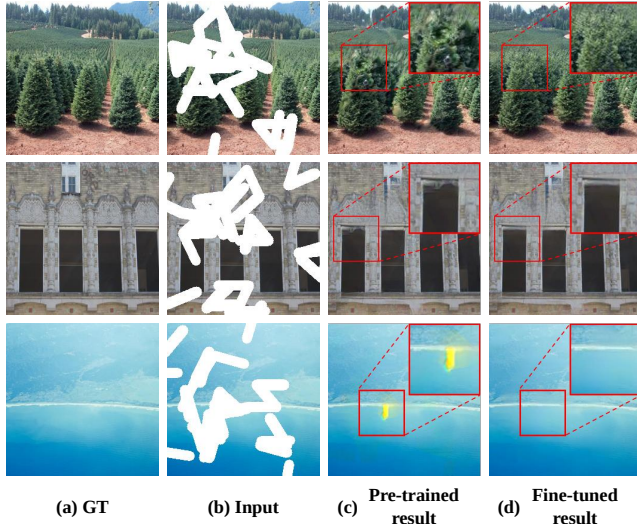


Figure 6: Qualitative comparison of results on the Places2 dataset before and after fine-tuning the pre-trained models.

tuning on the Urban100 test dataset. Although the initial results from the baseline models are poor since the Urban100 dataset is not used in pre-training the baseline networks, our fine-tuning results show considerable improvements by test-time adaptation. This finding proves that our fine-tuning method enhances the results although the input test image has a slightly different distribution from the dataset used in pre-training.

Qualitative results

We compare the qualitative results between the initially restored results by the pre-trained models and our results by fine-tuning the pre-trained baselines. Figure 6 shows visual results on the Places2 test dataset. Note that the generated part in the result images of pre-trained models is distorted or does not match the other part. By comparison, our fine-tuned models generate more natural results. Furthermore, the visual results are significantly improved when multiple repetitive patterns, such as windows and stairs, exist in the input image since the network is likely to learn the correct answer using many similar patches. The results on the Urban100 test dataset demonstrate improved performance for structural restoration due to the property of containing many repetitive structures within the image as shown in Figure 5.

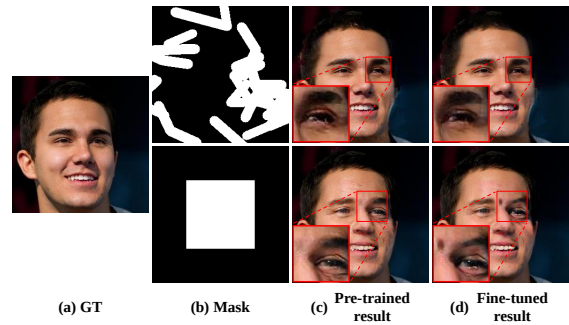


Figure 7: Results of Non-repetitive dataset. The result of the free-form mask that masks only one eye shows the improvement in the shape and color consistency of masked eye. On the other hand, the results of center mask shows the degradation in quality.

	Free-form mask	Center mask
PSNR	26.53 → 27.04	25.64 → 25.55
FID	29.48 → 28.19	31.03 → 31.79

Table 3: Comparisons between results before and after fine-tuning by GatedConv model on Celeba-HQ dataset.

Results from the non-repetitive images

We conduct experiments on Celeba-HQ (Karras et al. 2017) to show the result of our method from the non-repetitive facial input image with two different input masks: a central rectangle mask and a random free-form mask. Celeba-HQ is a large dataset including human faces, and we choose random 500 test images. We use the fully pre-trained GatedConv on the Celeba-HQ dataset. Figure 7 shows the comparison of before and after fine-tuning with two different shapes of masks. We can see improved eye shape and skin color consistency after fine-tuning when the input is corrupted by a free-form mask that includes one eye because the fine-tuned model can learn the self-similarity of the remaining part. However, when the input image is corrupted by a rectangle mask that covers two eyes, we can see the degraded result after fine-tuning. Table 3 indicates corresponding quantitative results.

Conclusion

A new self-supervision-based inpainting algorithm that allows the adaptation of fully pre-trained network parameters during the test stage is proposed. We utilize self-similar patches within the given input test image to fine-tune the network without using the ground-truth clean image and elevate the performance of networks by combining internal and large external information. We can easily fine-tune the baseline networks and significantly improve the performance over the baselines by optimizing loss functions, which are used to pre-train the baseline networks. The proposed method achieves state-of-the-art inpainting results on the conventional benchmark datasets, and extensive experimental results demonstrate the superiority of our method.

References

- Ballester, C.; Bertalmio, M.; Caselles, V.; Sapiro, G.; and Verdera, J. 2001. Filling-in by joint interpolation of vector fields and gray levels. *IEEE Transactions on Image Processing*, 10(8): 1200–1211.
- Barnes, C.; Shechtman, E.; Finkelstein, A.; and Goldman, D. B. 2009. PatchMatch: A randomized correspondence algorithm for structural image editing. *ACM Transactions on Graphics (ToG)*, 28(3): 24.
- Batson, J.; and Royer, L. 2019. Noise2Self: Blind Denoising by Self-Supervision. In *International Conference on Machine Learning (ICML)*.
- Bertalmio, M.; Sapiro, G.; Caselles, V.; and Ballester, C. 2000. Image inpainting. In *Proceedings of Conference on Computer graphics and Interactive Techniques*.
- Darabi, S.; Shechtman, E.; Barnes, C.; Goldman, D. B.; and Sen, P. 2012. Image Merging: Combining Inconsistent Images using Patch-based Synthesis. In *ACM Transactions on Graphics (SIGGRAPH)*.
- Glasner, D.; Bagon, S.; and Irani, M. 2009. Super-resolution from a single image. In *Proceedings of the IEEE International Conference on Computer Vision (ICCV)*.
- Goodfellow, I.; Pouget-Abadie, J.; Mirza, M.; Xu, B.; Warde-Farley, D.; Ozair, S.; Courville, A.; and Bengio, Y. 2014. Generative adversarial nets. In *Advances in Neural Information Processing Systems (NIPS)*.
- Hays, J.; and Efros, A. A. 2007. Scene completion using millions of photographs. *ACM Transactions on Graphics (TOG)*, 26(3): 4–es.
- Heusel, M.; Ramsauer, H.; Unterthiner, T.; Nessler, B.; and Hochreiter, S. 2017. Gans trained by a two time-scale update rule converge to a local nash equilibrium. In *Advances in Neural Information Processing Systems (NIPS)*.
- Huang, J.-B.; Kang, S. B.; Ahuja, N.; and Kopf, J. 2014. Image completion using planar structure guidance. *ACM Transactions on graphics (TOG)*, 33(4): 1–10.
- Huang, J.-B.; Singh, A.; and Ahuja, N. 2015. Single image super-resolution from transformed self-exemplars. In *Proceedings of the IEEE Conference on Computer Vision and Pattern Recognition (CVPR)*.
- Karras, T.; Aila, T.; Laine, S.; and Lehtinen, J. 2017. Progressive growing of gans for improved quality, stability, and variation. *arXiv preprint arXiv:1710.10196*.
- Kim, D.; Woo, S.; Lee, J.-Y.; and Kweon, I. S. 2019. Deep video inpainting. In *Proceedings of the IEEE Conference on Computer Vision and Pattern Recognition (CVPR)*.
- Krizhevsky, A. 2014. One weird trick for parallelizing convolutional neural networks. *arXiv preprint arXiv:1404.5997*.
- Lee, S.; Cho, D.; Kim, J.; and Kim, T. H. 2021. Restore from Restored: Single Image Denoising with Pseudo Clean Image. In *Proceedings of the IEEE Conference on Computer Vision and Pattern Recognition (CVPR)*.
- Lehtinen, J.; Munkberg, J.; Hasselgren, J.; Laine, S.; Karras, T.; Aittala, M.; and Aila, T. 2018. Noise2Noise: Learning Image Restoration without Clean Data. In *International Conference on Machine Learning (ICML)*.
- Levin, A.; Zomet, A.; Peleg, S.; and Weiss, Y. 2004. Seamless image stitching in the gradient domain. In *Proceedings of the European Conference on Computer Vision (ECCV)*.
- Li, J.; Wang, N.; Zhang, L.; Du, B.; and Tao, D. 2020. Recurrent Feature Reasoning for Image Inpainting. In *Proceedings of the IEEE Conference on Computer Vision and Pattern Recognition (CVPR)*.
- Liang, L.; Liu, C.; Xu, Y.-Q.; Guo, B.; and Shum, H.-Y. 2001. Real-time texture synthesis by patch-based sampling. *ACM Transactions on Graphics (ToG)*, 20(3): 127–150.
- Liu, G.; Reda, F. A.; Shih, K. J.; Wang, T.-C.; Tao, A.; and Catanzaro, B. 2018. Image inpainting for irregular holes using partial convolutions. In *Proceedings of the European Conference on Computer Vision (ECCV)*.
- Michaeli, T.; and Irani, M. 2014. Blind deblurring using internal patch recurrence. In *Proceedings of the European Conference on Computer Vision (ECCV)*.
- Nazeri, K.; Ng, E.; Joseph, T.; Qureshi, F.; and Ebrahimi, M. 2019. EdgeConnect: Structure Guided Image Inpainting using Edge Prediction. In *Proceedings of the IEEE International Conference on Computer Vision Workshops (ICCVW)*.
- Park, S.; Yoo, J.; Cho, D.; Kim, J.; and Kim, T. H. 2020. Fast Adaptation to Super-Resolution Networks via Meta-Learning. In *Proceedings of the European Conference on Computer Vision (ECCV)*.
- Pathak, D.; Krahenbuhl, P.; Donahue, J.; Darrell, T.; and Efros, A. A. 2016. Context encoders: Feature learning by inpainting. In *Proceedings of the IEEE Conference on Computer Vision and Pattern Recognition (CVPR)*.
- Ren, Y.; Yu, X.; Zhang, R.; Li, T. H.; Liu, S.; and Li, G. 2019. Structureflow: Image inpainting via structure-aware appearance flow. In *Proceedings of the IEEE International Conference on Computer Vision (ICCV)*.
- Shocher, A.; Cohen, N.; and Irani, M. 2018. “zero-shot” super-resolution using deep internal learning. In *Proceedings of the IEEE Conference on Computer Vision and Pattern Recognition (CVPR)*.
- Ulyanov, D.; Vedaldi, A.; and Lempitsky, V. 2018. Deep image prior. In *Proceedings of the IEEE conference on computer vision and pattern recognition*, 9446–9454.
- Wang, Y.; Tao, X.; Qi, X.; Shen, X.; and Jia, J. 2018. Image Inpainting via Generative Multi-column Convolutional Neural Networks. In *Advances in Neural Information Processing Systems (NIPS)*.
- Xiong, W.; Yu, J.; Lin, Z.; Yang, J.; Lu, X.; Barnes, C.; and Luo, J. 2019. Foreground-aware image inpainting. In *Proceedings of the IEEE Conference on Computer Vision and Pattern Recognition (CVPR)*.
- Xu, L.; Yan, Q.; Xia, Y.; and Jia, J. 2012. Structure extraction from texture via relative total variation. *ACM transactions on graphics (TOG)*, 31(6): 1–10.

Yu, J.; Lin, Z.; Yang, J.; Shen, X.; Lu, X.; and Huang, T. S. 2018. Generative image inpainting with contextual attention. In *Proceedings of the IEEE Conference on Computer Vision and Pattern Recognition (CVPR)*.

Yu, J.; Lin, Z.; Yang, J.; Shen, X.; Lu, X.; and Huang, T. S. 2019. Free-form image inpainting with gated convolution. In *Proceedings of the IEEE International Conference on Computer Vision (ICCV)*.

Zhang, R.; Isola, P.; Efros, A. A.; Shechtman, E.; and Wang, O. 2018. The unreasonable effectiveness of deep features as a perceptual metric. In *Proceedings of the IEEE Conference on Computer Vision and Pattern Recognition (CVPR)*.

Zhou, B.; Lapedriza, A.; Khosla, A.; Oliva, A.; and Torralba, A. 2017. Places: A 10 million image database for scene recognition. *IEEE Transactions on Pattern Analysis and Machine Intelligence (PAMI)*, 40(6): 1452–1464.

Zhou, T.; Tulsiani, S.; Sun, W.; Malik, J.; and Efros, A. A. 2016. View synthesis by appearance flow. In *Proceedings of the European Conference on Computer Vision (ECCV)*.